FULL PAPER DOI: 10.1002/adsc.202000514

Hydrophosphination of Activated Alkenes by a Cobalt(I) Pincer Complex

Roberto Nolla-Saltiel,[a] Ana M. Geer,[a, b,*] Laurence J. Taylor,[a] Olivia Churchill,[a] E. Stephen Davies,[a] William Lewis,[c] Alexander J. Blake,[a] and Deborah L. Kays[a,*]

[a] School of Chemistry, University of Nottingham, University Park, Nottingham, NG7 2RD, UK
E-mail: anageerramos@gmail.com; deborah.kays@nottingham.ac.uk
[b] Departamento de Química Inorgánica, Instituto de Síntesis Química y Catálisis Homogénea (ISQCH), CSIC Universidad de Zaragoza, Pedro Cerbuna 12, 50009 Zaragoza (Spain)
[c] School of Chemistry, The University of Sydney, F11, Eastern Ave, Sydney NSW 2006, Australia.

Manuscript received: April 28, 2020; Version of record online: June 3, 2020

Supporting information for this article is available on the WWW under https://doi.org/10.1002/adsc.202000514

Abstract: Herein we report the synthesis of three heteroleptic first-row transition metal(II) complexes containing carbazolido *NNN* pincer ligands and conversion to the corresponding metal(I)-carbonyl complexes *via* a reductive carbonylation route. These complexes are precatalysts for the hydrophosphination of activated alkenes, affording a cobalt-catalysed hydrophosphination process that solely and selectively yields the β addition (anti-Markovnikov) product. The scope of this transformation has been investigated using a variety of activated alkenes. Isolation and characterisation of substrate-coordinated intermediates reveal available coordination sites, which provide insight into the proposed catalytic cycle.

Keywords: Hydrophosphination; Activated Alkenes; First-Row Transition Metal; Pincer Complexes; Homogeneous Catalysis

Introduction

Phosphorus-containing compounds are a precious commodity, finding use in numerous areas such as organocatalysis,[1] bulk and fine chemical production,[2] and the pharmaceutical industry.[3] Aiming to access new synthetic routes for their preparation, these industries have stimulated the development of more effective, atom-economical routes and viable strategies for their preparation. However, a continuing challenge in this area is the ability to selectively and cleanly access compounds of interest.

Following our previous report, which detailed the use of low-coordinate transition metal precatalysts in the hydrophosphination of isocyanates,[4] we looked to extend our studies to other unsaturated substrates. Of special interest is the hydrophosphination of olefins and alkynes, which has received much attention in the last two decades.[5–11] The potential for accessing atom-efficient transformations involving regio- and stereoselective processes has, in turn, driven advances for metal-catalysed hydroelementation reactions. This has been revitalised by the development of tailored catalyst design; a core area for regioselective metal-catalysed hydrophosphination (Scheme 1). Furthermore, diminishing supplies of noble metals limits their future accessibility for catalysis,[12–14] and their relatively high toxicity encourages the reduction of their use in the synthesis of pharmaceuticals.[15] Therefore, the quest for cheaper, earth-abundant, non-toxic catalysts for hydrophosphination and other hetero-atom insertion processes, involving iron,[5,6,9,16–25] cobalt,[26–31] and manganese[32] is of continuing importance.

Selected examples of first row metal species employed in hydrophosphination include *β*-diketiminate iron(II) complexes capable of effecting the intramolecular hydrophosphination of alkenyl and phosphinoalkynes.[5] The regioselective, Lewis-acid

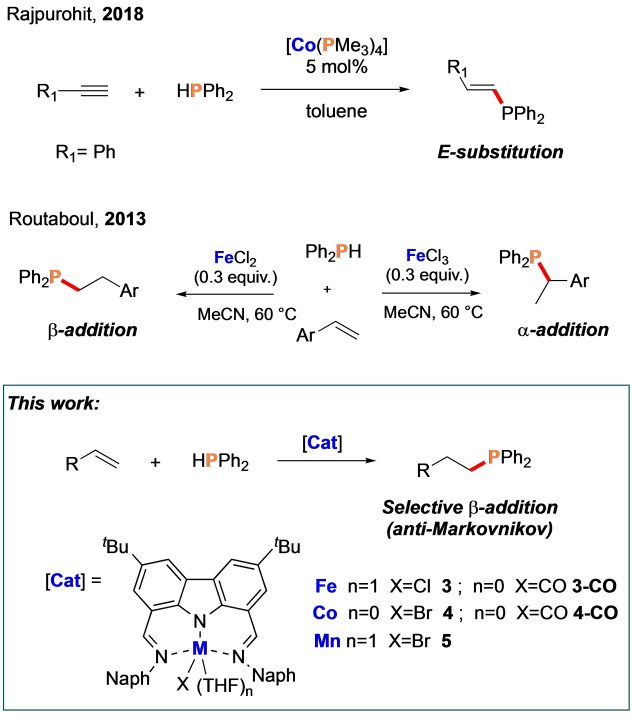

Scheme 1. Examples of first row transition-metal catalysed hydrophosphination of alkenes/alkynes.

directed substitution of diphenylphosphine on styrene derivatives selectively yields *α*- or *β*-hydroelementation products, dependent on the catalyst ($FeCl_3$ *vs.* $FeCl_2$).[9] The *E*-selective hydrophosphination of terminal and internal alkynes has also been catalysed by [Co(PMe_3)$_4$] (Scheme 1),[26] and manganese(II)-halides promote the hydrophosphination of 4-chlorostyrene.[32]

Notable examples of cobalt(II) complexes in the formation of new H-heteroatom bonds and C–H functionalisation include [Co(acac)$_2$] catalysed hydrophosphination of internal alkynes[27] and *Z*-selective hydrosilylation of terminal alkynes,[28] [*NNN*–$CoCl_2$] pincer-complexes active in regio- and enantio-selective hydrosilylation/hydrogenation of terminal alkynes,[30] $CoCl_2$-catalysed hydroamination of buta-1,3-dienes,[33] and a functionalised cobalt-salen complex active in the regioselective hydrothiolation of unactivated alkenes.[34] Examples of catalysis by cobalt(I)-metal centres include the orthoalkenylation of an azobenzene derivative with diphenylacetylene,[35] isomerisation-hydroboration of alkenes using [Co(H)(N_2)(PPh_3)$_3$],[36] piano-stool compounds [*e.g.* Cp*Co(CH_2=$CHSiMe_3$)$_2$] active in the inter- and intramolecular hydroacylation of olefins with aromatic[37] and aliphatic aldehydes,[38] the synthesis of enamines *via* intramolecular hydrogen transfer,[39] and chemoselective hydroboration of alkenes and nitriles employing a [*CCC*–CoN_2] pincer complex.[40]

Although the hydrophosphination of alkynes catalysed by cobalt-containing compounds is known,[26,27,41] there are no examples in which a cobalt catalyst has been employed in this transformation utilising olefinic substrates.

Results and Discussion

Synthesis of Transition Metal Complexes

We have recently described the use of sterically demanding carbazolido ligands based on 1,8-dinaphthylimino-3,6-di(*tert*-butyl)-9*H*-carbazole ($Naph_2carbH$, **1**) in the stabilisation of Group 1 metal centres [*e.g.* {$Naph_2carbK$}$_2$ (**2**)].[42] The [$Naph_2carb$]$^-$ ligand offers a strong *σ*-donor functionality,[43] and the incorporation of bulky substituents in the 1- and 8-positions offer a higher degree of protection around the central carbazolido-nitrogen, an essential feature for the formation of unsaturated and/or highly reactive metal centres.[44–46] Additionally, these salts are useful starting materials for the preparation of heteroleptic transition metal complexes. Compounds **3**–**5** were prepared *via* a metathesis reaction between the potassium salt **2** and an excess of $FeCl_2$·1.5THF (THF = tetrahydrofuran), $CoBr_2$·DME (DME = dimethoxyethane) and $MnBr_2$ in THF, affording [$Naph_2carbMX$(THF)] [MX=FeCl (**3**), MnBr (**5**)] or $Naph_2carbCoBr$ (**4**), respectively (Scheme 2). Pure samples of **3**–**5** were readily isolated following toluene extraction from the crude reaction mixture at room temperature (rt), with good to moderate yields of crystalline material (**3**, 52%; **4**, 86%; **5**, 51%), and have been characterised by structural and spectroscopic methods (Figure 1; see also Supporting Information, SI35–SI37, for further details).

From **3** and **4**, the metal(I)-carbonyl complexes could be formed by treatment with one equivalent of $LiBHEt_3$ and exposure of the *in situ* generated hydride complex (**3-H**/**4-H**) to an atmosphere of CO(g) (**3-CO** and **4-CO**; Scheme 2 and Figure 1).[47,48] Extraction of the reaction mixtures into toluene afforded **3-CO** and **4-CO**, allowing for characterisation by NMR spectro-

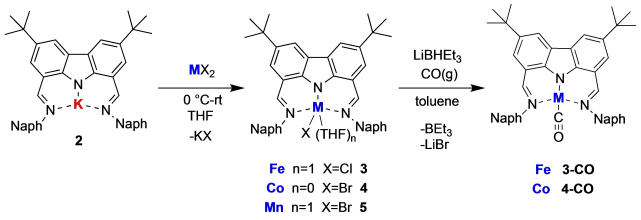

Scheme 2. Synthesis of first-row transition metal(II) complexes and reductive carbonylation to metal(I)-carbonyls. Synthesis and structure of the heteroleptic metal(II) complexes (**3**–**5**); reaction conditions (**2**: MX_2 = 1:2): 0 °C→rt, 48 h/MX_2 = $FeCl_2$·1.5THF (**3**), $CoBr_2$·DME (**4**), $MnBr_2$ (**5**). Synthesis of metal(I)-carbonyl complexes (**3-CO** and **4-CO**); reaction conditions: **3**/**4**:$LiBHEt_3$ = 1:1, excess CO(g), toluene, rt, 22 h. [Naph = 1-naphthyl].

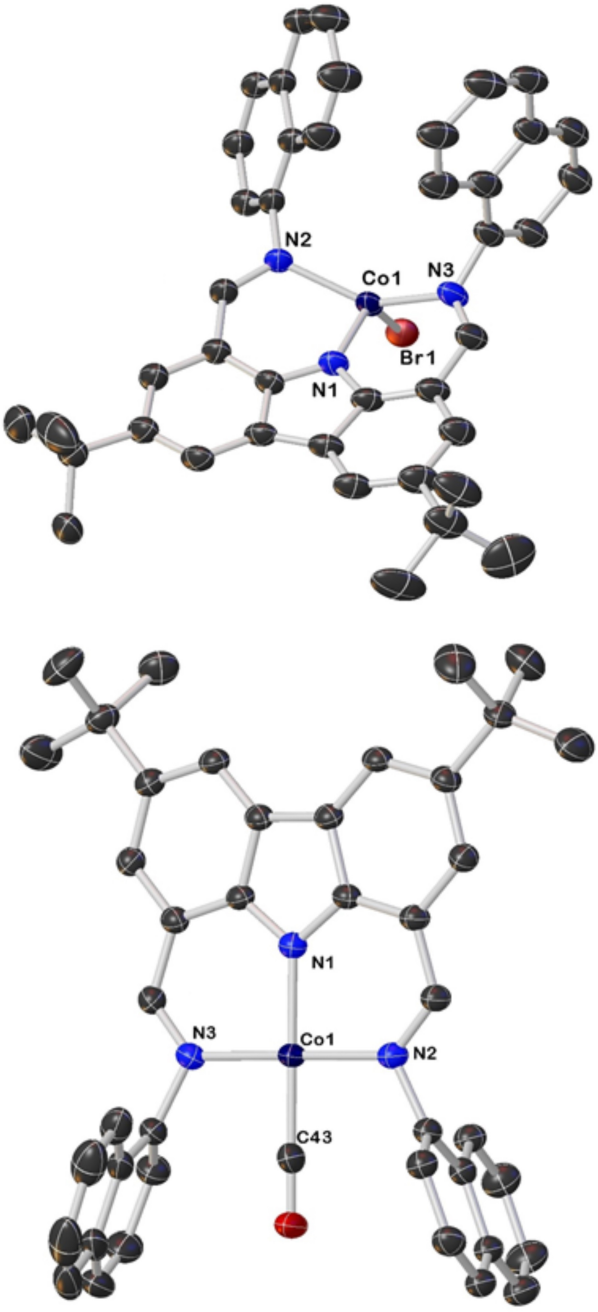

Figure 1. Molecular structures for one of the crystallographically independent molecules of **4** (*above*) and structure of **4-CO** (*below*), with anisotropic displacement ellipsoids set at 50% probability, and hydrogen atoms omitted for clarity. Selected bond lengths (Å) and angles (°) for **4**: Co1–Br1 2.3675(4); Co1–N1 1.906(2); Co1–N2 2.063(2); Co1–N3 2.046(2); N3–Co1–N2 140.54(8); N3–Co1–N1 90.31(7); N2–Co1–N1 90.97(7); N1–Co1–Br1 124.86(6). **4-CO**: Co1–C43 1.762(2); Co1–N1 1.887(2); Co1–N2 1.937(2); Co1–N3 1.947(2); N3–Co1–N2 179.47(7); N3–Co1–N1 90.12(7); N2–Co1–N1 90.40(7); N1–Co1–C43 179.22(11).

scopy, mass spectrometry, IR spectroscopy, and (for **4-CO**) single crystal X-ray diffraction (Figure 1). Samples of analytical purity were not obtained, and these carbonyl complexes were generated and utilised *in situ* for all subsequent catalytic reactions.

Catalytic Olefin Hydrophosphination and Reaction Optimisation

An initial assessment of the catalytic activity for the hydrophosphination of alkenes (Scheme 3, Table 1) was performed *via* the reaction of acrylonitrile with diphenylphosphine in C_6D_6 using 5 mol% of **3**, (Entry 3, Table 1). No evidence for the formation of hydrophosphination products was observed at rt. However, upon heating at 60 °C for 22 h, selective formation of the linear isomer (**A**, compound **10**) was observed (20% conversion). Heating for four days afforded *ca.* 50% conversion of the starting $HPPh_2$, with the linear isomer **A**, as the main product (49% *vs.* the branched isomer **B** 2%). Looking to aid deprotonation of $HPPh_2$, and to ensure the solubility of complex **3** (5 mol%) during catalysis, an excess of NEt_3 was added to the reaction. However, under these conditions, there was a decrease in conversion relative to the analogous experiment in absence of base (11% yield of the linear isomer, Entry 4, Table 1). However, the cobalt containing **4** exhibited a higher activity than iron containing **3** when NEt_3 was used as an additive (Entry 6, Table 1) giving 61% total conversion after 18 h, with an overall 58% yield of the linear isomer.

Under identical conditions, manganese complex **5** only achieved a 13% conversion after 18 hours, affording the β addition (anti-Markovnikov) isomer in 12% yield (Entry 7, Table 1). Returning to the more promising precatalyst **4**, increasing the reaction temperature to 80 °C afforded 88% conversion with the formation of the linear product in 74% yield (Entry 8, Table 1). The replacement of the bromide in **4** with a hydride was expected to increase the catalytic activity of the metal complex (Entry 9, Table 1).[30] However, the *in situ* generated hydride **4-H** exhibited decreased reactivity when compared with **4** under similar conditions (70% conversion after 22 h). Surprisingly, when the *in situ* generated cobalt(I)-carbonyl complex **4-CO** was tested in toluene, high conversions were achieved in < 2 h at 80 °C, with excellent (*ca.* 100%) selectivity for β-addition (Entry 10, Table 1, see SI31–SI32). The same reaction using the

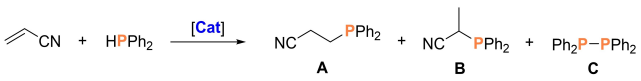

Scheme 3. Hydrophosphination of acrylonitrile with diphenylphosphine, depicting potential substitutions and dehydrocoupling products. [**Cat**] = **3**–**5**, **3-CO** and **4-CO**, **A** = β addition, **B** = α addition, **C** = dehydrocoupling product.

Table 1. Catalyst screening and reaction optimisation for the hydrophosphination of acrylonitrile.[a]

Entry	Catalyst (mol%)	Solvent	T (°C)	*t* (h)	Conv. (%)[d]	Product Ratio[d] **A**/**B**/**C**	Yield (%)[e]
1	–	C_6D_6	60	18	2	2/0/0	–
2	–[b]	C_6D_6	60	18	1	1/0/0	–
3	**3** (5)	C_6D_6	60	22	20	20/0/0	–
4	**3** (5)[b]	C_6D_6	60	22	11	11/0/0	–
5	**4** (5)	C_6D_6	60	17	40	39/0/1	–
6	**4** (5)[b]	C_6D_6	60	18	61	58/3/0	–
7	**5** (5)[b]	C_6D_6	60	18	13	12/1/0	–
8	**4** (5)[b]	Toluene	80	18	88	74/3/11	63
9	**4-H** (5)[c]	Toluene	80	22	70	68/2/0	–
10	**4-CO** (5)	Toluene	80	1.5	100	100/0/0	89
11	**3-CO** (5)	Toluene	80	17	59	37/7/15	27

[a] Reaction conditions: 5.0 mg of metal catalyst, 0.6 mL of solvent, 20 equiv. of acrylonitrile/$HPPh_2$. Samples were heated in an oil bath; progress was monitored by ^{31}P NMR spectroscopy.
[b] 20 equiv. of NEt_3 added; [M]:NEt_3, 1:20.
[c] 1 equiv. of Li[$BHEt_3$] added; [M]:Li[$BHEt_3$], 1:1.
[d] Determined by $^{31}P/^{31}P\{^1H\}$ NMR spectroscopy, product ratios given as % yield (based on substrate) of each isomer. **A** = β addition (anti-Markovnikov) product, **B** = α addition (Markovnikov) product, **C** = $Ph_2P–PPh_2$.
[e] Isolated yield as the phosphine oxide (**10a**). See **SI32** for reaction optimisation (NMR spectroscopy).

analogous iron complex (**3-CO**) only afforded a 59% conversion after 17 hours, with significant formation of the branched isomer **B** and the dehydrocoupling product **C** (Entry 11, Table 1). It is noteworthy that, whilst catalytic hydrophosphination of alkenes by first-row transition metals is known,[23,25,32] to our knowledge this is the first cobalt-based example. However, the analogous insertion in the more reactive alkynes is well documented for both hydrophosphination[26,27] and hydrosilylation.[29–31,49]

Based on the catalyst screening and optimisation experiments, it was decided to proceed using the conditions described in Entry 10 (Table 1). In order to determine the nature of the catalytic process, poisoning experiments with Hg[24,50] and CS_2,[4,51] were performed (Table SI1). No changes were observed in the reaction rate or product selectivity in the presence of Hg or CS_2 suggesting that the reaction most likely occurs through a homogenous mechanism. Moreover, the reaction does not appear to be radical mediated, since the presence of cumene[4,23,52,53] or 1,4-cyclohexadiene,[54,55] does not diminish the activity of the catalysts (Table SI1).

Substrate Scope

Having established complex **4-CO** as the most selective/active metal precatalyst, the reaction scope was investigated with a variety of activated unsaturated substrates. Results of the hydrophosphination reactions catalysed by cobalt(I) are shown in Table 2. Using an *α*-carbonyl unsaturated substrate such as methyl acrylate, the reaction reaches full conversion to the linear product **11** in 5 h (Entry 1, Table 2). Substitution of the α-carbon with a methyl group results in a significant drop in conversion (26%) despite prolonged reaction times (Entry 2, Table 2). This is most likely a consequence of steric hindrance. For activated non-terminal alkenes (fumaronitrile and dimethylfumarate) only the less sterically hindered fumaronitrile was susceptible to substitution, with full conversion to **13** in 1 h (Entry 3, Table 2). When the double bond was located in the *β*-position, even when activating functional groups are present (Table SI2, entries 5 and 6), no hydrophosphination was observed. It was noted that in all cases where coordination of the substrate to the catalyst is not possible, the dehydrocoupling product $Ph_2P–PPh_2$ (**C**) is obtained as the sole product. This suggests that, in substrates where hydrophosphination is unfavourable, an alternative pathway is enabled (*vide infra*) in which the stoichiometric transformation of $HPPh_2$ to $Ph_2P–PPh_2$ (**C**) occurs (See Table SI2). When vinylpyridines were used (Entries 4 and 5, Table 2), full conversion to the linear isomers (**14** and **15**) was achieved in 40 and 20 h, respectively. Similarly, the *α*-unsaturated ketone 2-cyclohexen-1-one gave selective substitution in the *β*-position with up to 81% conversion after 24 h (Entry 6, Table 2). In line with the reactivity described for Entries 1–3, a preference for activated terminal alkenes was observed when the isomeric lactones 5,6-dihydro-*2H*-pyran-2-one (Table SI2, entry 14) and *α*-methylene-γ-butyrolactone were employed, the latter yielding exclusively the β addition (anti-Markovnikov) product **17** in 4 h (Entry 7, Table 2). The low conversion of 5,6-dihydro-*2H*-pyran-2-one could be due to a combination of disfavoured attack at a secondary carbon, and the reduced electrophilicity of conjugated esters *vs.* alkenes (comparing to the sterically

Table 2. Summary of substrates susceptible to hydrophosphination catalysed by **4-CO**.

Entry	Substrate[a]	*t* (h)	Conv. (%)[b]	Product Ratio[b] **A**/**B**/**C**	Reaction Product	Yield (%)[c]
1	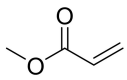	5	100	99/0/1	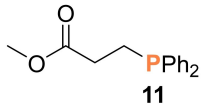 **11**	83
2	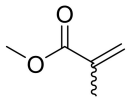	72	26	23/0/3	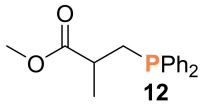 **12**	13
3	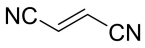	1	100	-/100/0	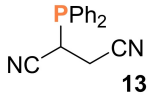 **13**	74
4	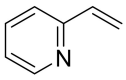	40	94	92/0/2	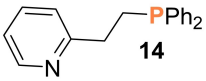 **14**	81
5	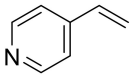	20	95	95/0/0	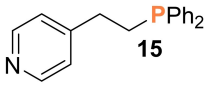 **15**	90
6	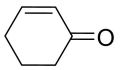	24	81	79/0/2	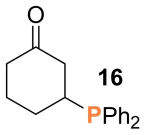 **16**	52[d]
7		4	86	86/0/0	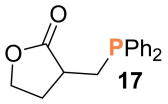 **17**	77
8	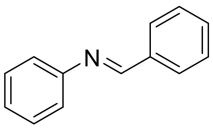	6	71	-/69/2	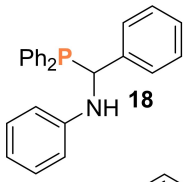 **18**	58
9	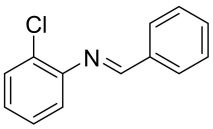	6	76	-/75/2	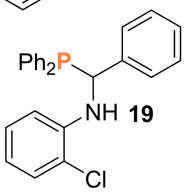 **19**	65
10	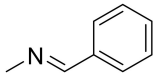	5	38	-/36/2	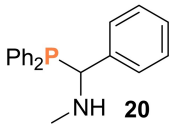 **20**	38[e]

[a] Reaction conditions: 5.0 mg, 6.92×10^{-3} mmol of **4-CO** (5 mol%), 0.6 mL of toluene, 20 equiv. of alkene/$HPPh_2$. Samples were heated in an oil bath at 80 °C, progress was monitored by NMR spectroscopy.

[b] Product ratios given as % yield (based on substrate) of each isomer as determined by $^{31}P/^{31}P\{^1H\}$ NMR spectroscopy. **A** = β addition (anti-Markovnikov) product, **B** = α addition (Markovnikov) product, **C** = Ph_2P–PPh_2.

[c] Isolated as the phosphine oxide.

[d] *β*-substituted product.

[e] Decomposes upon oxidation giving **20a** (see SI43). See Supplementary Information for full characterisation of all the hydrophosphination products, and a complete list of all substrates tested.

similar 2-cyclohexen-1-one). Aromatic imines (Entries 8 and 9, Table 2) are also substrates for substitution, with moderate conversions in under 6 hours. However, an aromatic imine with *ortho-i*Pr substituents was found to give no conversion under the same conditions (see Table SI2, entry 18). This may result from steric hindrance preventing coordination of the imine N to the catalyst. A methyl-substituted imine, by contrast, achieved relatively modest conversions when compared to the less bulky aryl imines (38% conversion in 5 h, Table 2, entry 10). This could be due to the more electron rich C=N bond disfavouring nucleophilic attack on the substrate.

For the initial steps in transition metal catalysed hydrophosphination reactions, two possible reaction pathways have been proposed. The first involves initial coordination of the secondary phosphine to the metal centre, yielding a metal-phosphide complex, and is favoured in systems catalysed by platinum,[56–61] lanthanides[62–65] and in some cases iron.[5,16] An alternative mechanism, involving the formation of a metal-olefin complex, is less common[66] and is most commonly reported for late first-row transition metals[9,67] and in limited cases by noble metals.[67–69] For analogous reactions involving the hydroamination of alkenes, the η^2-olefin is not directly activated upon coordination by the metal centre. Activation occurs when the olefin changes from η^2 to η^1 coordination and results in localisation of the LUMO for the ligand-M-{alkene} complex on the most distant carbon atom. This enhances the interaction with the incoming nucleophilic phosphine, as expected for phospha-Michael type reactions, a key feature in the reaction mechanism that explains the selective formation of β addition (anti-Markovnikov) product.[69–71]

Attempts to form a metal-phosphide complex between $HPPh_2$ and **4**/**4-CO** were unsuccessful, even when stoichiometric amounts of NEt_3 or $K[N(SiMe_3)_2]$ were employed. Nevertheless, we have been able to prepare and structurally characterise examples of metal-substrate complexes using **4** and the unsaturated substrates acrylonitrile (**6**), dimethyl fumarate (**8**) and methyl acrylate (**9**) (Figure 2 and SI39–SI42 for further details) to form five-coordinate compounds of general formula [Naph$_2$carbCo{substrate}Br] (**6–9**). In these, the substrate is bound to the metal *via* an electron-rich nitrogen or oxygen. These examples highlight the space available for coordination and reactivity around the low-coordinate metal centre.

Proposed Mechanism

The mechanism depicted in Scheme 4 attempts to reconcile our observations. Initially, **4-CO** coordinates the unsaturated substrate, forming the coordinated complex **I**, similar to complexes **6–9** (Scheme 4 and SI39–SI42). As it has been formally reduced, one

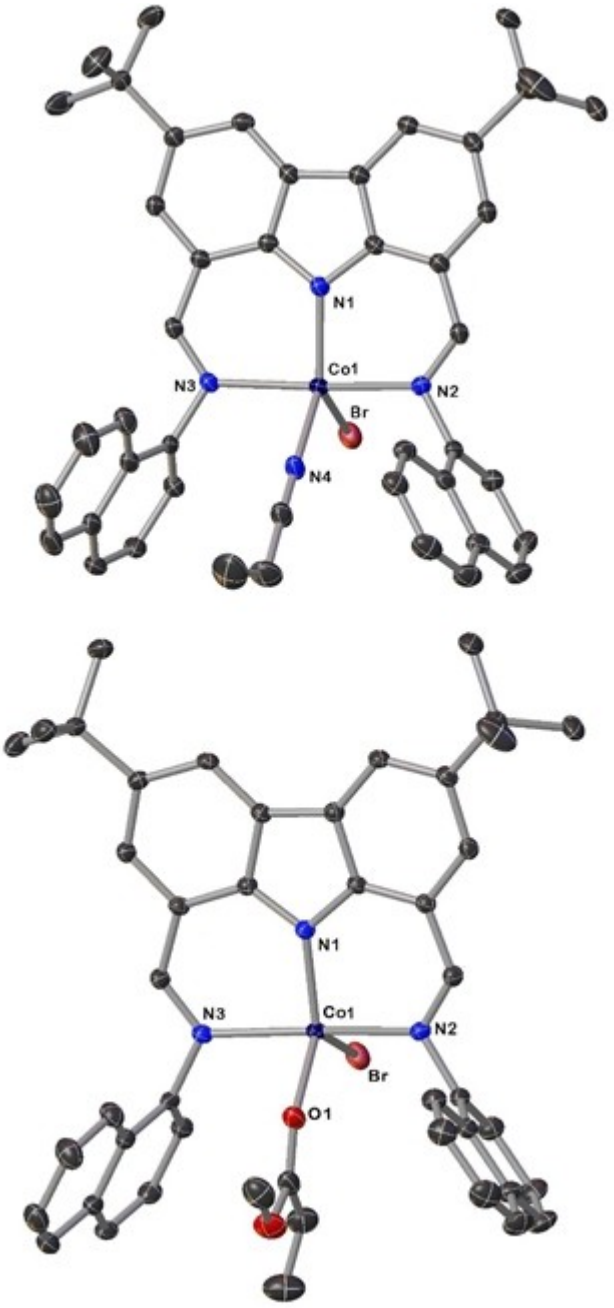

Figure 2. Molecular structure of **6** (*above*) and **9** (*below*), with anisotropic displacement ellipsoids set at 50% probability. Hydrogen atoms and solvent of crystallisation have been omitted for clarity. Selected bond lengths (Å) and angles (°) for **6**: Co1–Br1 2.4306(4); Co1–N4 2.0755(16); Co1–N1 1.9681(14); Co1–N2 2.2004(15); Co1–N3 2.1983(15); N3–Co1–N1 88.89(6); N2–Co1–N1 87.92(6); N1–Co1–Br1 116.44(5); N1–Co1–N4 137.20(7). **9**: Co1–Br1 2.4434(3); Co1–O1 2.0796(11); Co1–N1 1.9554(12); Co1–N2 2.1716(12); Co1–N3 2.1905(12); N3–Co1–N2 167.67(5); N3–Co1–N1 89.14(5); N2–Co1–N1 89.11(5); N1–Co1–Br1 116.87(4); N1–Co1–O1 125.17(5).

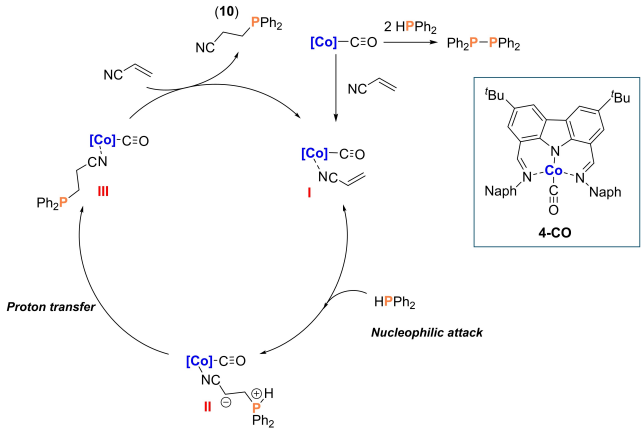

Scheme 4. Proposed reaction mechanism for the hydrophosphination of acrylonitrile, catalysed by **4-CO**.

might expect Co(I) species **4-CO** to be a weaker Lewis acid than Co(II) complex **4**. However, this is not necessarily the case, as **4-CO** has undergone a geometry change relative to **4** (square planar *vs.* seesaw) and a π-donating ligand (Br) replaced with a strong π-acceptor (CO). Indeed, there are several reports of Co(I) species behaving as Lewis acids under an appropriate ligand environment.[72–74]

Initial loss of carbon monoxide from the parent metal complex, *via* an initial carbonylation mechanism, is unlikely since NMR (^{1}H and ^{13}C{^{1}H}) studies show neither the formation of carbonylic products nor free CO and mass spectrometric determinations do not give molecular ions consistent with CO homologation into the substrate. This suggests that **4-CO** is the catalytically active species. After coordination, intermediate **I** undergoes nucleophilic substitution by the secondary phosphine (Michael addition). Kinetic determinations previously reported using an isostructural (four coordinate/square planar) and isolectronic (d^8), Ni(II) complex to **4-CO**, [Ni(κ^3-Pigiphos)(N≡CMeCCH$_2$)]$^{2+}$, have shown this initial step is reversible due to low energy barriers for nucleophilic attack and elimination by phosphines.[66] This step affords intermediate **II**, in a regioselective manner, with subsequent proton transfer to yield **III**. It should be noted that attempts to isolate and characterise intermediate **III**, or any of its analogues, were unsuccessful (stoichiometric reactions). This suggests that rapid elimination of product **10** occurs and regenerates the cobalt(I) catalyst (**4-CO**), which then coordinates an additional molecule of acrylonitrile, completing the catalytic cycle. An alternative reaction mechanism involving a Co(I)/Co(III) cycle, as proposed in some recent examples of cobalt hydrofunctionalisation reactions,[75,76] cannot be ruled out with our experimental data; with current investigations in our group targeting a detailed analysis of the reaction mechanism for this transformation. Finally, our catalytic experiments show that for reactions where a metal-olefin complex cannot be formed, or if the unsaturated substrate is too sterically hindered or inactive (*e.g.* styrene), then the reaction produces stoichiometric quantities of the dehydrocoupling product, $Ph_2P–PPh_2$. A similar observation has been previously reported by Webster *et al.*, in processes catalysed by *β*-diketiminate iron complexes.[5,21]

Conclusions

We have reported the synthesis and characterisation of three heteroleptic metal(II) *NNN* pincer complexes. From these, two metal(I)-carbonyl complexes have been prepared using a reductive carbonylation process. All of these complexes are catalytically active in the hydrophosphination of activated olefins, with the cobalt(I) carbonyl complex showing significant promise for this reaction. The method has been extended to a range of substrates, yielding selective β addition (anti-Markovnikov) products. Experiments to characterise the mechanism by which the reaction takes place has allowed us to draw similarities with equivalent heteroatom insertion reactions, founded in crystallographically authenticated analogues.

Experimental Section

Apart from the synthesis of the ligand (Naph$_2$carbH, **1**) and the phosphine oxides, all products described were treated with rigorous exclusion of air and water using standard air-sensitive handling techniques which included bench-top operations (Schlenk line) and glove-box techniques. NMR samples of air and moisture sensitive compounds were prepared using glove box techniques and contained in Young's tap modified borosilicate glass NMR tubes. NMR data were collected on either a Bruker DPX300, DPX400, AV400, AV(III)400, AV(III) 400HD or AV(III)600 spectrometer. Chemical shifts are quoted in ppm relative to TMS (^{1}H, ^{13}C{^{1}H}) and H_3PO_4 (^{31}P, ^{31}P{^{1}H}). Reaction progress was monitored by quantitative ^{31}P, ^{31}P{^{1}H} NMR spectroscopy (inverse gated decoupled) of samples prepared in dry, non-deuterated toluene, with a C_6D_6 insert for locking. Apart from the substrates employed in Entries 8–9, Table 2, which were prepared following reported procedures;[77] all reagents were used as received. Magnetic moments were calculated through the Evans method at 298 K, employing C_6D_6 as solvent. Diamagnetic corrections were calculated according to Pascal's constants.[78] CCDC 1874664-1874672 contain the supplementary data for **3**–**9**, **4-CO** and **20a**. These data can be obtained free of charge from The Cambridge Crystallographic Data Centre via www.ccdc.cam.ac.uk/data_request/cif. **Safety warnings**: 1-Naphthylamine is highly toxic and is suspected to be a carcinogen; great care must be taken during synthesis and adequate handling of waste should be procured. Carbon monoxide is an extremely toxic and flammable gas, good ventilation within a fumehood should be procured when running a Schlenk line with this gas as source, away from open flames and with a carbon monoxide detector operating at all times.

Solutions containing Li[BHEt$_3$] (Super-Hydride®), are extremely pyrophoric and flammable upon exposure to air, ensuring handling of this compound under inert conditions is paramount.

Synthesis of Heteroleptic Metal(II) Complexes (3–5)

Typical procedure: A Schlenk flask containing **1** (500 mg, 0.85 mmol) and KH (68 mg, 1.71 mmol, 2 eq.) was cooled to 0 °C and THF (50 mL) was slowly added. The resulting suspension was stirred at 0 °C for 1 hour and subsequently allowed to warm to rt with stirring over 3 hours. The dark red suspension of **2** was cooled to 0 °C and filtered/dropwise added to a suspension of the desired metal(II) dihalide (MX_2) (1.71 mmol, 2 eq.) {*vide infra*}. The resulting mixture was allowed to warm up to rt overnight and then stirred for 48 hours. The volatiles were removed under vacuum and the residue was extracted into toluene (20 mL × 3). The resulting solution was evaporated *in vacuo*, affording the desired products (**3–5**) as powders. Crystals suitable for XRD for **3–5**, were grown from concentrated hexane solutions at rt.

1,8-Dinaphthylimino-3,6-Di(tert-butyl)-9-Fe–(THF)–Cl-Carbazole (3)

MX_2=$FeCl_2 \cdot 1.5THF$. ^{1}H NMR (400 MHz, C_6D_6) [all peaks appear as broad singlets] δ 57.28 ($\Delta\nu_{1/2}$ = 350 Hz), 20.48 ($\Delta\nu_{1/2}$ = 365 Hz), 10.83 ($\Delta\nu_{1/2}$ = 225 Hz), 8.52 ($\Delta\nu_{1/2}$ = 75 Hz), 6.10 ($\Delta\nu_{1/2}$ = 118 Hz), 2.12 ($\Delta\nu_{1/2}$ = 47 Hz), 1.47 ($\Delta\nu_{1/2}$ = 80 Hz), 0.31 ($\Delta\nu_{1/2}$ = 50 Hz), −2.60 ($\Delta\nu_{1/2}$ = 226 Hz), −3.73 ($\Delta\nu_{1/2}$ = 197 Hz), −16.13 ($\Delta\nu_{1/2}$ = 273 Hz), −25.54 ($\Delta\nu_{1/2}$ = 427 Hz). HRMS/ASAP *m/z*: $[M-Cl-C_4H_8O]^+$ calculated 638.2462, found 638.2460 formula $C_{42}H_{38}N_3Fe$. Anal. Calcd for $C_{46}H_{46}ClFeN_3O$: C 73.85, H 6.20, N 5.62; Found C 73.99, H 6.12, N 5.48. IR ν/cm^{-1} (Nujol): 2958, 2855, 1666, 1570, 1554, 1507, 1461. μ_{eff} (Evans, C_6D_6, 25 °C) = 3.33 μ_B. UV/vis (toluene, c = 2.67 × 10^{-5} mol dm^{-3}): λ_{max}/nm ($\varepsilon \times 10^3$/dm^3 mol^{-1} cm^{-1}) 386 (9.29). Dark red-brown powder (131 mg, 52%).

1,8-Dinaphthylimino-3,6-Di(tert-butyl)-9-Co–Br-Carbazole (4)

MX_2 = $CoBr_2 \cdot DME$. ^{1}H NMR (400 MHz, C_6D_6) [all peaks appear as broad singlets] δ 46.94 ($\Delta\nu_{1/2}$ = 160 Hz), 22.06 (&bkM$\Delta\nu_{1/2}$ = 206 Hz), 4.74 ($\Delta\nu_{1/2}$ = 111 Hz), 2.13 ($\Delta\nu_{1/2}$ = 89 Hz), 1.37 ($\Delta\nu_{1/2}$ = 141 Hz), 1.02 ($\Delta\nu_{1/2}$ = 62 Hz), 0.32, −0.38 ($\Delta\nu_{1/2}$ = 83 Hz), −2.76 ($\Delta\nu_{1/2}$ = 104 Hz), −15.69 ($\Delta\nu_{1/2}$ = 130 Hz), −18.25 ($\Delta\nu_{1/2}$ = 239 Hz), −64.21 ($\Delta\nu_{1/2}$ = 2179 Hz). HRMS/ASAP *m/z*: $[M]^+$ calculated 722.1581, found 722.1597 formula $C_{42}H_{38}N_3BrCo$. Anal. Calcd for $C_{42}H_{38}BrCoN_3$: C 69.71, H 5.29, N 5.81; Found C 69.56, H 5.11, N 5.65. IR ν/cm^{-1} (Nujol): 2956, 2921, 2854, 1545, 1461. μ_{eff} (Evans, C_6D_6, 25 °C) = 2.92 μ_B. UV/vis (toluene, c = 1.38 × 10^{-5} mol dm^{-3}): λ_{max}/nm ($\varepsilon \times 10^3$/dm^3 mol^{-1} cm^{-1}) 386 (9.91). Bright purple powder (530 mg, 86%).

1,8-Dinaphthylimino-3,6-Di(tert-butyl)-9-Mn–(THF)–Br-Carbazole (5)

MX_2 = $MnBr_2$. ^{1}H NMR (400 MHz, C_6D_6) [all peaks appear as broad singlets] δ 22.08 ($\Delta\nu_{1/2}$ = 1437 Hz), 13.40 ($\Delta\nu_{1/2}$ = 25 Hz), 8.51 ($\Delta\nu_{1/2}$ = 27 Hz), 6.52 ($\Delta\nu_{1/2}$ = 27 Hz), 2.11 ($\Delta\nu_{1/2}$ = 61 Hz), 1.49 ($\Delta\nu_{1/2}$ = 29 Hz), 0.30 ($\Delta\nu_{1/2}$ = 27 Hz), −8.95 ($\Delta\nu_{1/2}$ = 808 Hz). Anal. Calcd for $C_{46}H_{46}BrMnN_3O$: C 69.78, H 5.86, N 5.31; Found C 68.51, H 5.74, N 4.90. Despite repeated attempts, a satisfactory elemental analysis for this compound could not be obtained. This is likely a consequence of its very high sensitivity or due to partial loss of coordinating solvent, prior to analysis.[79–81] MS/ASAP *m/z*: $[M-C_4H_8O-Br]^+$ calculated 639.2446, found 639.2454 formula $C_{42}H_{38}N_3Mn$. IR ν/cm^{-1} (Nujol): 2955, 2926, 2854, 1631, 1599, 1571, 1482, 1461. μ_{eff} (Evans, C_6D_6, 25 °C) = 3.64 μ_B. UV/vis (toluene, c = 2.53 × 10^{-5} mol dm^{-3}): λ_{max}/nm ($\varepsilon \times 10^3$/dm^3 mol^{-1} cm^{-1}) 386 (14.48). Dark pink-orange powder (135 mg, 51%).

Typical Procedure for the Formation of Metal(I) Complexes (Reductive Carbonylation; 3-CO and 4-CO) For Catalytic Scale Reactions

In a glovebox, **3** (5 mg, 6.68 × 10^{-3} mmol) or **4** (5 mg, 6.92 × 10^{-3} mmol) was dissolved in dry toluene (0.6 mL). The resulting dark purple solution was transferred to a Young's tap modified borosilicate glass NMR tube. Shortly after, $LiBHEt_3$ (1 M solution in THF, 7 µL, 7 × 10^{-3} mmol) was added to the NMR tube rendering the solution black. The NMR tube was sealed, removed from the glovebox and connected to a Schlenk line running on CO(g). The tubing connecting the NMR tube to the line was thoroughly cycled before the tube was opened and the atmosphere within the tube was replaced with CO(g) *via* three freeze-pump-thaw cycles. The resulting mixture was left under this atmosphere for 22 hours. Crystals suitable for XRD, for **4-CO**, were grown in a glovebox from a saturated C_6D_6 solution *via* hexane vapour diffusion, at rt.

1,8-Dinaphthylimino-3,6-Di(tert-butyl)-9-Fe–CO-Carbazole (3-CO)

^{1}H NMR (400 MHz, C_6D_6) [all peaks appear as broad singlets] δ 45.41 ($\Delta\nu_{1/2}$ = 452 Hz), 3.66 ($\Delta\nu_{1/2}$ = 124 Hz), 2.12 ($\Delta\nu_{1/2}$ = 72 Hz), 1.46 ($\Delta\nu_{1/2}$ = 89 Hz), 1.12 ($\Delta\nu_{1/2}$ = 41 Hz), 0.95 ($\Delta\nu_{1/2}$ = 354 Hz), 0.29 ($\Delta\nu_{1/2}$ = 51 Hz), −23.11 ($\Delta\nu_{1/2}$ = 193 Hz). MS/ASAP *m/z*: $[M-CO]^+$ calculated 638.2454, found 638.2462 formula $C_{42}H_{38}N_3Fe$. IR ν/cm^{-1} (toluene): 2020, 1999, 1976, 1909 (C≡O). [Repeated attempts at growing crystals of **3-CO** suitable for study by single X-ray diffraction were unsuccessful. Despite this, multinuclear structures relying on bridging carbonyls have been ruled out, due to absence of characteristic υ_{CO} signals at lower wavenumber (1800–1500 cm^{-1})]. Brown powder (14.8 mg, 55%, see ESI for large-scale synthesis).

1,8-Dinaphthylimino-3,6-Di(tert-butyl)-9-Co–CO-Carbazole (4-CO)

^{1}H NMR (400 MHz, C_6D_6) [all peaks appear as broad singlets] δ 56.04 ($\Delta\nu_{1/2}$ = 198 Hz), 22.53 ($\Delta\nu_{1/2}$ = 209 Hz), 15.55 ($\Delta\nu_{1/2}$ = 178 Hz), 8.94 ($\Delta\nu_{1/2}$ = 93 Hz), 8.44 ($\Delta\nu_{1/2}$ = 94 Hz), 5.67 ($\Delta\nu_{1/2}$ =

140 Hz), 4.07 ($\Delta\nu_{1/2}$ = 129 Hz), 1.66 ($\Delta\nu_{1/2}$ = 106 Hz), 0.96 ($\Delta\nu_{1/2}$ = 130 Hz), 0.30 ($\Delta\nu_{1/2}$ = 84 Hz), −12.38 ($\Delta\nu_{1/2}$ = 160 Hz), −13.96 ($\Delta\nu_{1/2}$ = 177 Hz), −52.6 ($\Delta\nu_{1/2}$ = 944 Hz). HRMS/ASAP *m/z*: $[M-CO]^+$ calculated 643.2398, found 643.2402 formula $C_{42}H_{38}N_3Co$. IR ν/cm^{-1} (toluene): 3649, 3439, 2012, 1908 (C≡O). Black powder (34.8 mg, 75%, see ESI for large-scale synthesis).

Typical Procedure for the Hydrophosphination of Activated Alkenes

To a solution of the isolated or *in situ* generated **4-CO** (5 mg, 6.92×10^{-3} mmol) in toluene (with C_6D_6 insert), acrylonitrile (9.06 µL, 0.138 mmol, 20 eq.) and then $HPPh_2$ (24 µL, 0.138 mmol, 20 eq.) were added. The resulting NMR sample was transferred to an oil bath set at the desired temperature (Table 1 and Table 2) and the reaction was monitored until the resonances attributed to the starting material disappeared (^{31}P NMR spectroscopy) or when no significant reaction progress was observed (**10**). In order to isolate the hydrophosphination products, the reaction mixtures were purposely oxidised (**10a**).[16] In all cases the crude mixture was opened to air and added to a silica gel plug (petroleum ether 40–60) to remove the unreacted $HPPh_2$. The product was eluted with Et_2O, this fraction was exposed to H_2O_2 (30% w/w, 5 mL) and stirred at rt for 10 min. The reaction mixture was quenched with deionised water and the organic phase was separated, dried over $MgSO_4$ and evaporated. In the particular case of products **15a** and **16a**, the crude product after oxidation with H_2O_2, was extracted with CH_2Cl_2 due to the increased solubility of the products in H_2O. For full characterisation of the hydrophosphination products, see the supporting information.

Acknowledgements

This work was supported by the Engineering and Physical Sciences Research Council [grant number EP/R004064/1]; The Leverhulme Trust [grant number RPG-2014-317]; CONACYT (Mexican Council for Science and Technology) [grant number CVU 600474] and the University of Nottingham. We also thank the EPSRC UK National Mass Spectrometry Facility at Swansea University and Dr Mick Cooper (University of Nottingham) for mass spectrometry, Mr Stephen Boyer (London Metropolitan University) for elemental analyses and Dr Huw Williams (University of Nottingham) for helpful NMR discussions.

References

[1] J. L. Methot, W. R. Roush, *Adv. Synth. Catal.* **2004**, *346*, 1035–1050.
[2] H. Pellissier, H. Clavier, *Chem. Rev.* **2014**, *114*, 2775–2823.
[3] D. W. Allen, *Organophosphorus Chem.* **2016**, *45*, 1–50.
[4] H. R. Sharpe, A. M. Geer, W. Lewis, A. J. Blake, D. L. Kays, *Angew. Chem. Int. Ed.* **2017**, *56*, 4845–4848; *Angew. Chem.* **2017**, *129*, 4923–4926.
[5] M. Espinal-Viguri, A. K. King, J. P. Lowe, M. F. Mahon, R. L. Webster, *ACS Catal.* **2016**, *6*, 7892–7897.
[6] M. Itazaki, S. Katsube, M. Kamitani, H. Nakazawa, *Chem. Commun.* **2016**, *52*, 3163–3166.
[7] A. Di Giuseppe, R. De Luca, R. Castarlenas, J. J. Pérez-Torrente, M. Crucianelli, L. A. Oro, *Chem. Commun.* **2016**, *52*, 5554–5557.
[8] C. A. Bange, R. Waterman, *ACS Catal.* **2016**, *6*, 6413–6416.
[9] L. Routaboul, F. Toulgoat, J. Gatignol, J. F. Lohier, B. Norah, O. Delacroix, C. Alayrac, M. Taillefer, A. C. Gaumont, *Chem. Eur. J.* **2013**, *19*, 8760–8764.
[10] A. M. Geer, A. L. Serrano, B. De Bruin, M. A. Ciriano, C. Tejel, *Angew. Chem. Int. Ed.* **2015**, *54*, 472–475; *Angew. Chem.* **2015**, *127*, 482–485.
[11] P. E. Sues, A. J. Lough, R. H. Morris, *J. Am. Chem. Soc.* **2014**, *136*, 4746–4760.
[12] S. Asghar, S. B. Tailor, D. Elorriaga, R. B. Bedford, *Angew. Chem. Int. Ed.* **2017**, *56*, 16367–16370; *Angew. Chem.* **2017**, *129*, 16585–16588.
[13] H. M. O'Brien, M. Manzotti, R. D. Abrams, D. Elorriaga, H. A. Sparkes, S. A. Davis, R. B. Bedford, *Nat. Catal.* **2018**, *1*, 429–437.
[14] A. M. Messinis, S. L. J. Luckham, P. P. Wells, D. Gianolio, E. K. Gibson, H. M. O'Brien, H. A. Sparkes, S. A. Davis, J. Callison, D. Elorriaga, O. Hernandez-Fajardo, R. B. Bedford, *Nat. Catal.* **2019**, *2*, 123–133.
[15] Guideline on the Specification Limits for Residues of Metal Catalysts or Metal Impurities EMA/CHMP/ICH353369/2013 **2016**.
[16] A. K. King, K. J. Gallagher, M. F. Mahon, R. L. Webster, *Chem. Eur. J.* **2017**, *23*, 9039–9043.
[17] J. R. F. Pritzwald-Stegmann, P. Lönnecke, E. Hey-Hawkins, *Dalton Trans.* **2016**, *45*, 2208–2217.
[18] M. Kamitani, M. Itazaki, C. Tamiya, H. Nakazawa, *J. Am. Chem. Soc.* **2012**, *134*, 11932–11935.
[19] J. Sugiura, T. Kakizawa, H. Hashimoto, H. Tobita, H. Ogino, *Organometallics* **2005**, *24*, 1099–1104.
[20] A. J. Price, P. G. Edwards, *Chem. Commun.* **2000**, *3*, 899–900.
[21] A. K. King, A. Buchard, M. F. Mahon, R. L. Webster, *Chem. Eur. J.* **2015**, *21*, 15960–15963.
[22] J. S. Huang, G. A. Yu, J. Xie, K. M. Wong, N. Zhu, C. M. Che, *Inorg. Chem.* **2008**, *47*, 9166–9181.
[23] K. J. Gallagher, R. L. Webster, *Chem. Commun.* **2014**, *50*, 12109–12111.
[24] C. A. Brown, T. A. Nile, M. F. Mahon, R. L. Webster, *Dalton Trans.* **2015**, *44*, 12189–12195.
[25] K. J. Gallagher, M. Espinal-Viguri, M. F. Mahon, R. L. Webster, *Adv. Synth. Catal.* **2016**, *358*, 2460–2468.
[26] J. Rajpurohit, P. Kumar, P. Shukla, M. Shanmugam, M. Shanmugam, *Organometallics* **2018**, *37*, 2297–2304.
[27] H. Ohmiya, H. Yorimitsu, K. Oshima, *Angew. Chem. Int. Ed.* **2005**, *44*, 2368–2370; *Angew. Chem.* **2005**, *117*, 2420–2422.
[28] W. J. Teo, C. Wang, Y. W. Tan, S. Ge, *Angew. Chem. Int. Ed.* **2017**, *56*, 4328–4332; *Angew. Chem.* **2017**, *129*, 4392–4396.
[29] J. Sun, L. Deng, *ACS Catal.* **2016**, *6*, 290–300.

[30] J. Guo, X. Shen, Z. Lu, *Angew. Chem. Int. Ed.* **2017**, *56*, 615–618; *Angew. Chem.* **2017**, *129*, 630–633.
[31] J. Guo, Z. Lu, *Angew. Chem. Int. Ed.* **2016**, *55*, 10835–10838; *Angew. Chem.* **2016**, *128*, 10993–10996.
[32] A. Leyva-Pérez, J. A. Vidal-Moya, J. R. Cabrero-Antonino, S. S. Al-Deyab, S. I. Al-Resayes, A. Corma, *J. Organomet. Chem.* **2011**, *696*, 362–367.
[33] R. Baker, A. Onions, R. J. Popplestone, T. N. Smith, *J. Chem. Soc. Perkin Trans. 1* **1975**, 1133–1138.
[34] V. Girijavallabhan, C. Alvarez, F. G. Njoroge, *J. Org. Chem.* **2011**, *76*, 6442–6446.
[35] G. Halbritter, F. Knoch, A. Wolski, H. Kisch, *Angew. Chem. Int. Ed.* **1994**, *33*, 1603–1605; *Angew. Chem.* **1994**, *106*, 1676–1678.
[36] M. L. Scheuermann, E. J. Johnson, P. J. Chirik, *Org. Lett.* **2015**, *17*, 2716–2719.
[37] C. P. Lenges, M. Brookhart, *J. Am. Chem. Soc.* **1997**, *119*, 3165–3166.
[38] C. P. Lenges, P. S. White, M. Brookhart, *J. Am. Chem. Soc.* **1998**, *120*, 6965–6979.
[39] A. D. Bolig, M. Brookhart, *J. Am. Chem. Soc.* **2007**, *129*, 14544–14545.
[40] A. D. Ibrahim, S. W. Entsminger, A. R. Fout, *ACS Catal.* **2017**, *7*, 3730–3734.
[41] K. Gao, N. Yoshikai, *Acc. Chem. Res.* **2014**, *47*, 1208–1219.
[42] R. Nolla-Saltiel, A. M. Geer, W. Lewis, A. J. Blake, D. L. Kays, *Chem. Commun.* **2018**, *54*, 1825–1828.
[43] M. A. W. Lawrence, K.-A. Green, P. N. Nelson, S. C. Lorraine, *Polyhedron* **2018**, *143*, 11–27.
[44] A. J. Blake, W. Lewis, J. McMaster, R. S. Moorhouse, G. J. Moxey, D. L. Kays, *Dalton Trans.* **2011**, *40*, 1641–1645.
[45] R. S. Moorhouse, G. J. Moxey, F. Ortu, T. J. Reade, W. Lewis, A. J. Blake, D. L. Kays, *Inorg. Chem.* **2013**, *52*, 2678–2683.
[46] F. Ortu, G. J. Moxey, A. J. Blake, W. Lewis, D. L. Kays, *Chem. Eur. J.* **2015**, *21*, 6949–6956.
[47] L. Wu, Q. Liu, R. Jackstell, M. Beller, *Angew. Chem. Int. Ed.* **2014**, *53*, 6310–6320; *Angew. Chem.* **2014**, *126*, 6426–6436.
[48] N. Hazari, J. E. Heimann, *Inorg. Chem.* **2017**, *56*, 13655–13678.
[49] J. Guo, X. Shen, Z. Lu, *Angew. Chem. Int. Ed.* **2017**, *56*, 615–618; *Angew. Chem.* **2017**, *129*, 630–633.
[50] G. M. Whitesides, M. Hackett, R. L. Brainard, J.-P. P. M. Lavalleye, A. F. Sowinski, A. N. Izumi, S. S. Moore, D. W. Brown, E. M. Staudt, *Organometallics* **1985**, *4*, 1819.
[51] B. J. Hornstein, J. D. Aiken, R. G. Finke, *Inorg. Chem.* **2002**, *41*, 1625–1638.
[52] A. Malekafzali, K. Malinovska, F. W. Patureau, *New J. Chem.* **2017**, *41*, 6981–6985.
[53] Y. Moglie, M. J. González-Soria, I. Martín-García, G. Radivoy, F. Alonso, *Green Chem.* **2016**, *18*, 4896–4907.
[54] Y. Miller, L. Miao, A. S. Hosseini, S. R. Chemler, *J. Am. Chem. Soc.* **2012**, *134*, 12149–12156.
[55] J. A. Hawari, P. S. Engel, D. Griller, *Int. J. Chem. Kinet.* **1985**, *17*, 1215–1219.
[56] E. Costa, P. G. Pringle, M. B. Smith, K. Worboys, *J. Chem. Soc. Dalton Trans.* **1997**, 4277–4282.
[57] P. G. Pringle, M. B. Smith, *Chem. Commun.* **1990**, 1701–1702.
[58] D. K. Wicht, I. V. Kourkine, B. M. Lew, J. M. Nthenge, D. S. Glueck, *J. Am. Chem. Soc.* **1997**, *119*, 5039–5040.
[59] D. K. Wicht, I. V. Kourkine, I. Kovacik, D. S. Glueck, *Organometallics* **1999**, *18*, 5381–5394.
[60] I. Kovacik, D. K. Wicht, N. S. Grewal, D. S. Glueck, C. D. Incarvito, I. A. Guzei, A. L. Rheingold, *Organometallics* **2000**, *19*, 950–953.
[61] L. Rosenberg, *ACS Catal.* **2013**, *3*, 2845–2855.
[62] M. R. Douglass, M. Ogasawara, S. Hong, M. V. Metz, T. J. Marks, *Organometallics* **2002**, *21*, 283–292.
[63] A. M. Kawaoka, M. R. Douglass, T. J. Marks, *Organometallics* **2003**, *22*, 4630–4632.
[64] A. M. Kawaoka, T. J. Marks, *J. Am. Chem. Soc.* **2004**, *126*, 12764–12765.
[65] A. M. Kawaoka, T. J. Marks, *J. Am. Chem. Soc.* **2005**, *127*, 6311–6324.
[66] A. D. Sadow, A. Togni, *J. Am. Chem. Soc.* **2005**, *127*, 17012–17024.
[67] M. A. Kazankova, M. O. Shulyupin, I. P. Beletskaya, *Synlett* **2003**, *2*, 2155–2158.
[68] F. Jerome, F. Monnier, H. Lawicka, S. Derien, P. H. Dixneuf, *Chem. Commun.* **2003**, *6*, 696–697.
[69] A. Couce-Rios, A. Lledós, G. Ujaque, *Chem. Eur. J.* **2016**, *22*, 9311–9320.
[70] O. Eisenstein, R. Hoffmann, *J. Am. Chem. Soc.* **1980**, *102*, 6148–6149.
[71] O. Eisenstein, R. Hoffmann, *J. Am. Chem. Soc.* **1981**, *103*, 4308–4320.
[72] N. K. Kildahl, W. J. Clark, *J. Coord. Chem.* **1992**, *25*, 291–297.
[73] N. K. Kildahl, P. Viriyanon, *Inorg. Chem.* **1987**, *26*, 4188–4194.
[74] A. Z. Spentzos, C. L. Barnes, W. H. Bernskoetter, *Inorg. Chem.* **2016**, *55*, 8225–8233.
[75] K. Duvvuri, K. R. Dewese, M. M. Parsutkar, S. M. Jing, M. M. Mehta, J. C. Gallucci, T. V. Rajanbabu, *J. Am. Chem. Soc.* **2019**, *141*, 7365–7375.
[76] T. Michiyuki, K. Komeyama, *Asian J. Org. Chem.* **2020**, *9*, 343–358 .
[77] A. Hasegawa, Y. Naganawa, M. Fushimi, K. Ishihara, H. Yamamoto, *Org. Lett.* **2006**, *8*, 3175–3178.
[78] D. F. Evans, *J. Chem. Soc.* **1959**, 2003–2005.
[79] J. Zou, D. J. Berg, A. Oliver, B. Twamley, *Organometallics* **2013**, *32*, 6532–6540.
[80] R. J. Less, H. R. Simmonds, S. B. J. Dane, D. S. Wright, *Dalton Trans.* **2013**, *42*, 6337–6343.
[81] S. K. Yen, L. L. Koh, F. E. Hahn, H. V. Huynh, T. S. A. Hor, *Organometallics* **2006**, *25*, 5105–5112.

